RSC Advances

Preparation and characterization of KGM-g-St/BA fibers and core/shell PCL/KGM-g-St/BA fibers

Journal:	*RSC Advances*
Manuscript ID:	RA-ART-12-2014-016170.R1
Article Type:	Paper
Date Submitted by the Author:	12-Feb-2015

Complete List of Authors:	Zhu, Jiuya; School of Materials Science and Engineering, Southwest University of Science and Technology, Engineering Research Center of Biomass Materials, Ministry of Education, Mianyang 621010, Sichuan, China xiaoyan, lin; Southwest University of Science and Technology, Zhang, zhongqing; School of Materials Science and Engineering, Southwest University of Science and Technology, Engineering Research Center of Biomass Materials, Ministry of Education Luo, Xuegang; Southwest University of Science and Technology, Engineering Research Center of Biomass Materials, Ministry of Education

Preparation and characterization of KGM-g-St/BA fibers and core/shell PCL/KGM-g-St/BA fibers

Jiuya Zhu[a,b], Xiaoyan Lin [a,b,*], Zhongqing Zhang [a,b] ,Xuegang Luo [b]

[a] *School of Materials Science and Engineering, Southwest University of Science and Technology, Mianyang 621010, Sichuan, China*

[b] *Engineering Research Center of Biomass Materials, Ministry of Education, Mianyang 621010, Sichuan, China*

Abstract

In order to improve the spinnability and develop a potential application of konjac glucomannan (KGM), KGM grafted with styrene (St)/butyl acrylate (BA) (KGM-g-St/BA) was prepared via free-radical polymerization in this study. Subsequently, fibers of KGM-g-St/BA and core-shell poly(caprolactone) (PCL) /KGM-g-St/BA fibers were respectively obtained by electrospinning technique. The property of KGM-g-St/BA copolymer and fibers were characterized by FTIR, TG, SEM, FE-SEM and TEM. The hydrophobic property of KGM has dramatically increased via grafting modification. KGM-g-St/BA graft copolymer fiber film and core-shell fiber film have a good hydrophobic property.

Keywords: konjac glucomannan; grafting modification; electrospinning; poly(caprolactone); coaxial electrospinning

1 Introduction

Electrospinning technique is a simple and effective approach to produce polymeric nano/submicron scale fibers with an extremely high surface area, high porosity with very small pore size and uniform fiber diameter [1-3]. Therefore, electrospun polymer fibers have been applied in a vast number of areas, such as filtration [4], nanocomposite [5], biomedical material [6], electronic component [7] and so on. Coaxial electrospinning is a branch technology of electrospinning [8], which is a simple technique to produce core /shell fibers ranging from 0.1 to 10 μm in diameter by employing two concentric spinnerets (“needles”) to feed fluids to a coaxially jetting stream [9]. The material properties could be enhanced via core/shell

* Corresponding author. Tel: +86 0816 6089372, Fax: +86 0816 6089372.
Email address: lxy20100205@163.com (X. Lin)

structures obtained by coaxial electrospinning [10-11]. Until now, many kinds of natural and synthetic polymers or graft copolymers have been prepared into micro/nanofibers by electrospinning and coaxial electrospinning [12-13].

KGM was a high-molecular weight water-soluble and non-ionic polysaccharides [14], composed of β-(1→4) linked D-glucose and D-mannose in a molar ratio of 1.6:1 with a low degree of acetyl groups [15]. It could be extracted from tubers of amorphophallus konjac plant in large quantities [16], which was a kind of cheap, renewable and biodegradable natural plant polysaccharides, had wide applications in food [17-18], chemical, medical [19], drug delivery [20], coating and encapsulation [21] and so on. It had attracted great interest in the field of electrospinning since had excellent film-forming ability, good biocompatibility and biodegradability [14]. However, the electrospinning of pure KGM was still difficult because its aqueous solution contained long chain molecular entanglement and extensive hydrogen bonding network. Furthermore, the electrospinning of KGM was carried out by means of blending with other materials mainly in the literature [22]. Hence chemical modification of KGM, such as esterification [23], deacetylation, [19], nitration [24], etherification [25], and graft polymerization [24, 26], was an effective and important method to improve its spinnability. Different properties of polymer monomer could be introduced to the structure via graft modification [27-29]. To date, electrospinning of KGM graft copolymer has not been reported. In order to improve the spinnability, KGM was grafted with St and BA via free-radical polymerization using ammonium persulfate (APS) as an initiator in this study. Up to now, the research about electrospun fibers of modified KGM was rarely reported and the synthesis of chemical modification of KGM with St and BA has not yet been reported.

PCL had received much attention due to its high flexibility and biodegradability as well as its hydrophobic nature [30]. Combining the advantages of PCL, in order to develop more application of KGM, core/shell bicomponent fibers of PCL and KGM-g-St/BA were prepared by coaxial electrospinning.

In order to improve the spinnability of KGM and develop a potential application of KGM, in this study, a novel chemical modification copolymer (KGM-g-St/BA) was prepared and fibers of KGM-g-St/BA copolymers and core-shell PCL/KGM-g-St/BA fibers were successfully obtained by electrospinning technique. Further, the KGM-g-St/BA copolymers and fibers were characterized by fourier transform infrared spectroscopy (FT-IR), thermogravimetric analysis (TGA), scanning electron microscopy (SEM), field emission scanning electron microscope (FE-SEM), transmission electron microscopy (TEM), and surface tensiometer.

2 Experimental

2.1. Materials

Konjac glucomannan (Mn = 8.38×10^5) was purchased from Mianyang Anxian Dule Company and was used without further purification. The chemicals of experiment inclusive of poly(caprolactone) (PCL) (Mn = 80,000), styrene (St), butyl acrylate (BA), ammonium persulfate (APS) and trifluoroacetic acid (TFA) were all of analytical grade and obtained from Chengdu Kelong Chemicals Company.

2.2. Methods

2.2.1. Synthesis of KGM-g-St/BA copolymer

3 g KGM and 150 mL distilled water were added into the three-necked round bottom flask equipped with a mechanical stirrer and a condenser putting in water bath pot of constant temperature under the protection of nitrogen, stirred for 30 min at 80 ^{o}C. Then an initiator of 0.2 g APS, 7.5 g of St and 7.5 g of BA added into the flask, and stirred for 3.5 h at 70 ^{o}C. Finally, the reaction mixture was poured into 300 mL of ethanol to precipitate the grafted copolymer. The precipitate was filtered, washed thoroughly with ethanol, and dried in an oven at 60 ^{o}C. Soxhlet extraction with toluene was applied to extract the homopolymer of St and BA in the graft copolymers at 120 ^{o}C for 24 h, the complete extraction was confirmed when no precipitation in the extracted solution was observed after dropped into ethanol. The graft copolymers was dried in a vacuum oven at 60 ^{o}C until a constant weight and kept in the desiccator.

2.2.2. Preparation of KGM-g-St/BA copolymer fibers by electrospinning

The electrospinning setup (DT-1003) was purchased from Dalian Ding Tong Technology Development Co., Ltd (Dalian, China), which comprised a high-voltage DC power (Tianjin Dongwen high-voltage power supply Co., Ltd), a syringe pump, and an iron plate collector. The electrospinning solution of 6 wt% concentration was prepared by dissolving KGM-g-St/BA powder in TFA, then stored at room temperature for 30 min before electrospinning. The fibers were collected on tin foil placed the iron plate collector with spinning conditions as follows: 5 wt% KGM-g-St/BA solution, the conducted voltage of 10-30 kV, a flow rate was operated on 0.5-2.5 mL/h, the distance was varied in the range of 9-21 cm, the needle inner diameter was ranging from 6 to 12$^{\#}$, the electrospinning temperature was varied in the range of 20-40 ^{o}C.

2.2.3. Preparation of core/shell PCL/KGM-g-St/BA fibers by coaxial eletrospinning

PCL solution of 5 wt% concentration was prepared by dissolving the polymer in TFA with magnetic stirring for 6 h at room temperature and ultrasonic de-airbubbling for 20 min in the ultrasonator. The method to prepare KGM-g-St/BA solution of 6 wt% concentration was the same as PCL solution of 5 wt% concentration. Core/shell PCL/KGM-g-St/BA fibers by coaxial eletrospinning, which using $12^{\#}$ stainless steel syringe needle as shell spinneret and $6^{\#}$ stainless steel syringe needle as core spinneret, were obtained from the following condition: 1 $mL \cdot h^{-1}$ of feeding rate of KGM-g-St/BA shell spinning solution, 0.5 $mL \cdot h^{-1}$ of feeding rate of PCL core spinning solution, 15 kV of voltage, 30 ^{o}C of spinning temperature and 15 cm of tip-to-collector distance.

2.3. Characterization

FT-IR spectroscopy of KGM and KGM-g-St/BA samples were measured in the range 400-4000 cm^{-1} by infrared spectrophotometer (Nicolet 6700, USA) using method of KBr pellets.

The sample of 5 mg KGM or KGM-g-St/BA copolymer was characterized by TGA (TA-Q500, USA) at a heating rate of 10 ^{o}C/min under a constant nitrogen atmosphere (traffic: 90 ml/min) with a range of temperature from 25 to 630 ^{o}C.

The morphology of KGM-g-St/BA copolymer fibers with gold coating was observed by SEM (Hitichi TM-3000, Japan) at different electrospinning parameters. In order to measure the average fiber diameters and diameter distribution of KGM-g-St/BA fibers for each sample, 50 fibers were randomly selected from SEM images of each sample and their average fiber diameters were measured using Image-J image processing software. The cross-section morphology of core/shell PCL/KGM-g-St/BA fibers was characterized by FE-SEM (Ultra 55, Carl Zeiss, Germany). The core/shell structure of PCL/KGM-g-St/BA fibers was characterized by TEM (Zeiss Libra 200F, Germany).

Water contact angles (WCA) of disks and electrospun films were tested by surface tensiometer (Sigma70, Finland), immediately after deionized water was fallen freely onto the surface of the disks or film. The WCA in each case was recorded in six measurements as the average of the values at three locations spacing 5 mm on each sample.

3 Results and discussion

3.1 FT-IR and TGA analysis

FT-IR spectra of the KGM and KGM-g-St/BA were shown in Fig. 1a. The FT-IR spectrum of KGM-g-St/BA copolymer contained all the characteristics of absorption peaks of KGM, such as the stretching vibration of O-H groups of the methyl at 3400 cm^{-1} , C-H at 2926 cm^{-1}, acetyl C=O at 1730 cm^{-1} [31], C-O at 1060 cm^{-1} [32]. Furthermore, it could be seen that the characteristic absorption peaks of benzene ring in the KGM-g-St/BA appear at 3027, 1543, 1493, 1453, 760 and 700cm^{-1}. The peak of KGM-g-St/BA at 3027 cm^{-1} was attributed to C–H stretching vibration of the benzene ring, the bands at 1543, 1493 and 1453 cm^{-1} owing to the skeletal C=C vibration and peaks at 760 and 700 cm^{-1} were the styrene ring out of plane deformation [33]. The peak of KGM-g-St/BA at 1155 cm^{-1} was the C-O-C asymmetric stretching vibration of butyl acrylate [34]. In comparison of the absorption peak of KGM and KGM-g-St/BA, it was evident that an enhanced absorption peak at 1730cm^{-1} existed in KGM-g-St/BA, coming from C=O stretching of butyl acrylate.

Fig. 1b showed the thermogravimetric curve of KGM, St/BA and KGM-g-St/BA, the weight loss of KGM in the range of 25-100 ºC was owing to the evaporation of moisture in the sample, and the maximum weight loss of about 80% for KGM began at 300 ^{o}C was attributed to thermal decomposition, while the weight loss of about 99.5% for St/BA began at 420 ^{o}C might be related to the degradation of St/BA. For the grafted KGM-g-St/BA, two thermal decomposition steps could be clearly observed, the first stage attributed to the decomposition of KGM skeleton between 240 and 400 ºC with the weight loss of 40%, the second stage was due to the chain decomposition of the graft copolymer of St/BA between 400 and 500 ºC with the weight loss of 40%. It was observed that the initial decomposition temperature of KGM-g-St/BA was significantly lower than that of KGM, probably ascribed to the hydrogen bonds and chemical bonds in the structure of KGM were destroyed after grafting of St and BA monomers, resulting in degradation of KGM molecule chains. Both FT-IR and TGA analysis confirmed that KGM grafted with St/BA (KGM-g-St/BA) was successfully synthesized.

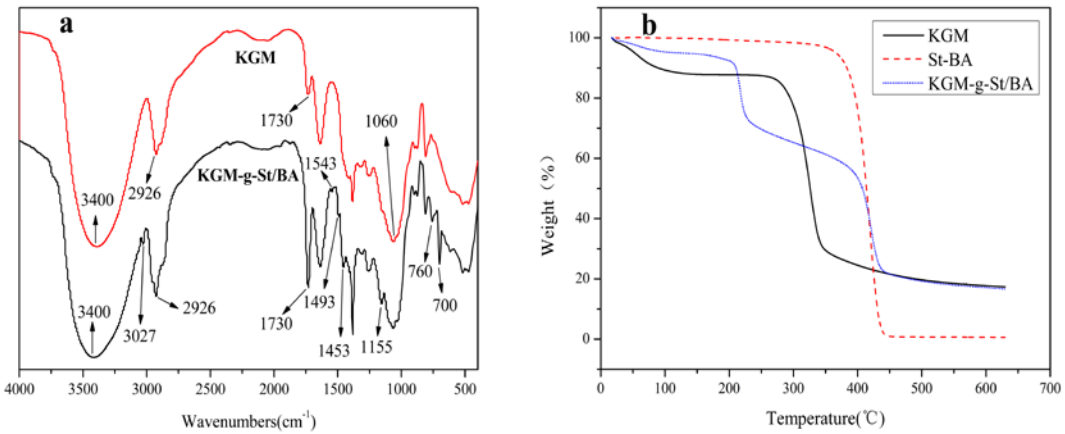

Fig. 1. (a) FT-IR spectra of KGM and KGM-g-St/BA and (b) TGA thermogram of KGM, St-BA copolymer and KGM-g-St/BA copolymer.

3.2 Effects of electrospinning parameters on morphology of KGM-g-St/BA copolymer fibers

3.2.1 Influence of voltage

In the electrospinning process, the strength of the voltage controlled formation of fibers from several microns to tens of nanometers in diameter [35]. Only after attainment of threshold voltage, fiber formation occurred, this induced the necessary charges on the solution along with electric field and initiated the electrospinning process [36]. It could be observed that voltage in the range of 10-30 kV had an effect on average diameters and diameter distribution of fibers from Fig. 2, the average fiber diameters decreased from 855.3 nm to 590.3 nm and the diameter distribution was concentrated from 400-1400 nm to 400-800 nm with the increasing of applied voltage. The possible reason was that a higher voltage caused greater stretching of the solution due to the greater columbic forces in the jet as well as a stronger electric field and these effects leaded to reduction in the fiber diameters and also rapid evaporation of solvent from the fibers results [36].

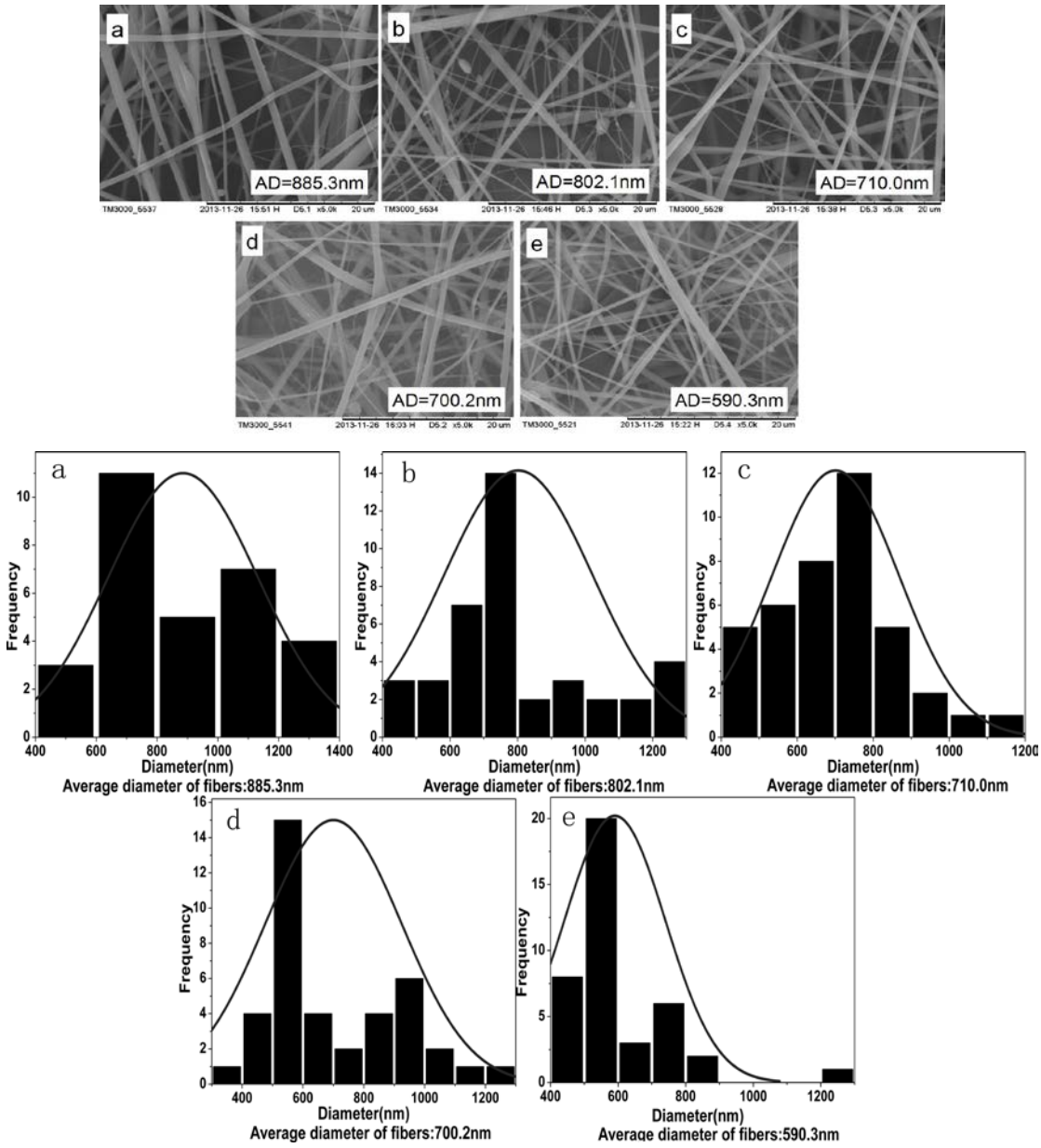

Fig. 2. SEM images and diameter distribution of KGM-g-St/BA fibers at various applied voltage (a) 10 kV, (b) 15 kV, (c) 20 kV, (d) 25 kV, (e) 30 kV; 1 mL/h , 15 cm, 8#, 35 ºC.

3.2.2 Influence of flow rate

The flow rate of the polymer solution was an important process parameter as it influenced the jet velocity and the material transfer rate [36]. This might have a significant impact on the morphology of the fibers. Fig. 3(a-e) showed the SEM images and diameter distribution of fibers at different flow rates. It could be observed that the fiber diameter, diameter distribution and the morphological structure could be slightly altered by changing the flow rate, average fiber diameters increased gradually from 582.0 nm to 809.2 nm as the flow rate increased due to the solvent of polymer solution would get enough time for evaporation at a lower flow rate [36]. While the

diameter distribution of fibers varied from mostly around 400 nm to 700 nm and was broaden at the flow rate of 2.5 mL/h, probably due to a high flow rate caused the instability in jet.

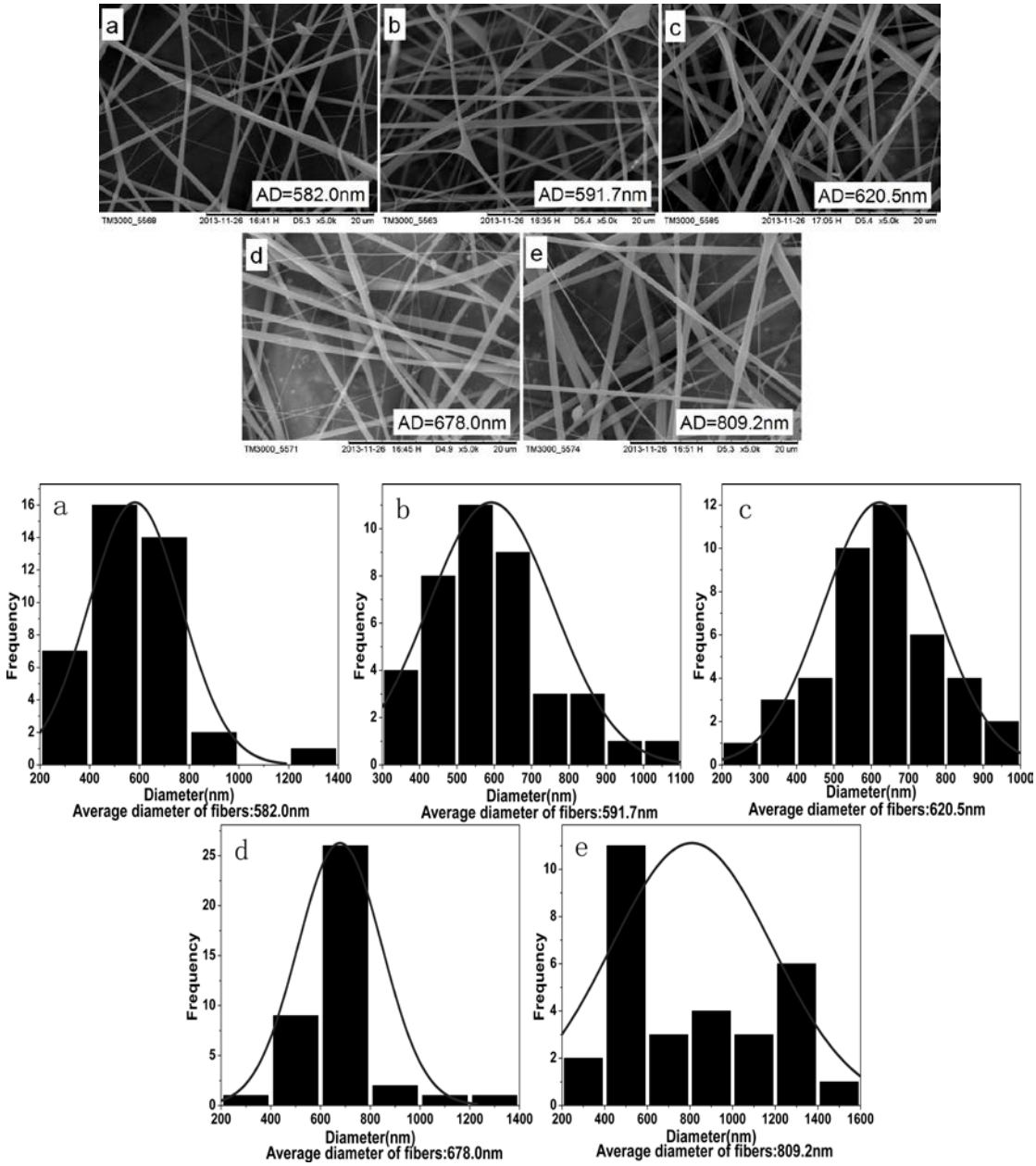

Fig. 3. SEM images and diameter distribution of KGM-g-St/BA fibers at various flow rate (a) 0.5 mL/h, (b) 1 mL/h, (c) 1.5 mL/h, (d) 2 mL/h, (e) 2.5 mL/h; 15 kV, 15 cm, 8#, 35 ºC.

3.2.3 Influence of needle tip to collector distance

Varying the distance between needle tip and collector would have a dual influence in both fiber diameters and morphology. The electric field strength would increase as the distance decreased. As a result, fiber diameter decreased. However, reduced the distance would also lead to not complete evaporation of solvent and this would increase the diameter of the fibers [37]. Fig. 4(a-e) showed the SEM images of

fibers and diameter distribution at various needle tips to collector distance. Increasing the distance resulted in an increase of the average fiber diameters from 610.6 nm to 762.2 nm and the range of diameter distribution of fibers changed from 300-1100 nm to 200-1800 nm. This was due to a weaker electrostatic field caused less stretching of the solution because of a greater distance of needle tip to collector, which leaded to an increase in the fiber diameter and broadening of diameter distribution.

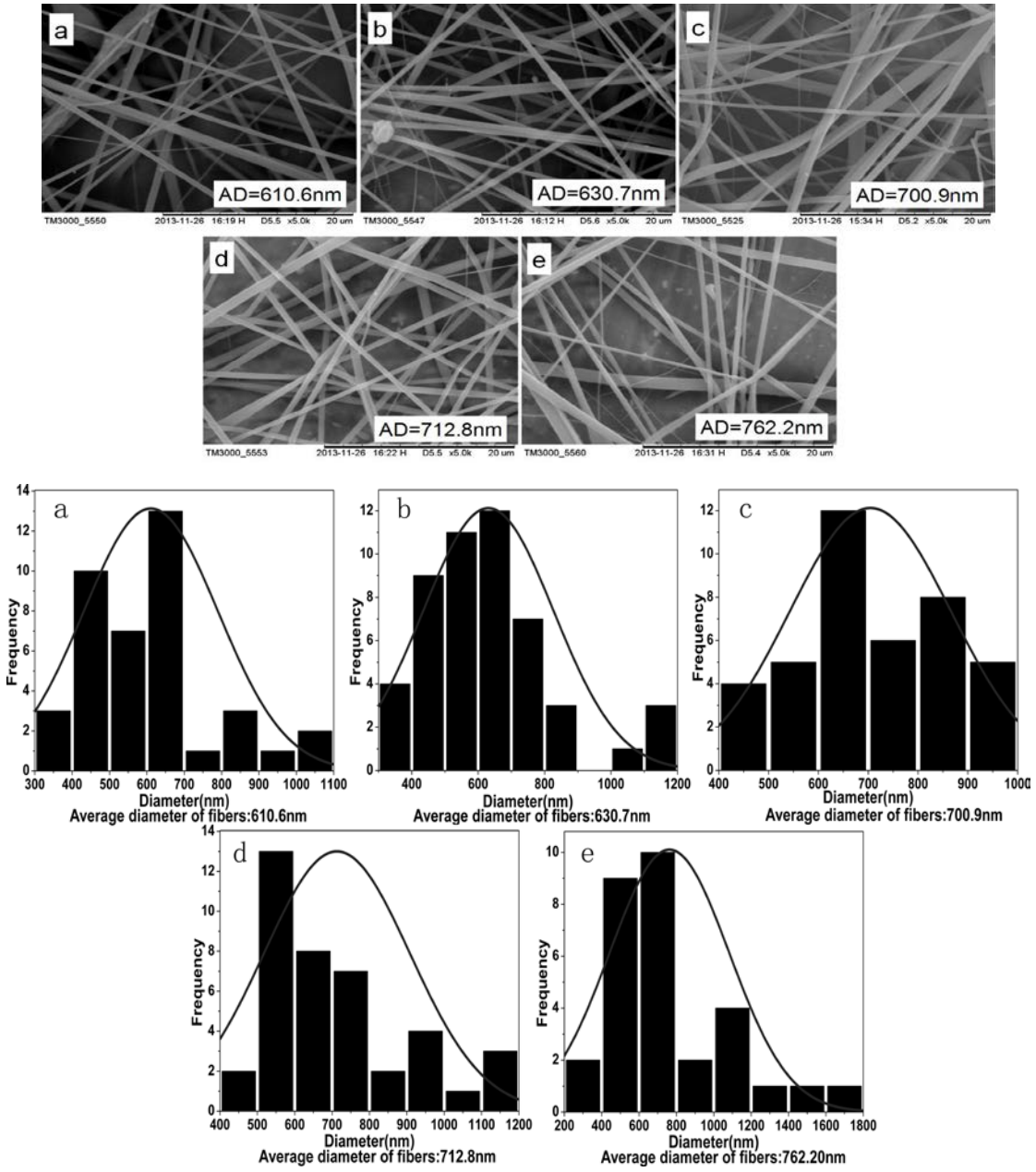

Fig. 4. SEM images and diameter distribution of KGM-g-St/BA fibers at various needle tip to collector distance (a) 9 cm, (b) 12 cm, (c) 15 cm, (d) 18 cm, (e) 21cm; 15 kV, 1 mL/h, 15 cm, 8#, 35 ºC.

3.2.4 Influence of the needle inner diameter

The inner diameter of the needle has been examined as another parameter to influence the morphology and average diameter of fibers. The average fiber diameters increased from 695.93 nm to 967.13 nm with an increase in the needle inner diameter and relatively wide fiber diameter distribution of 200-2000 nm was seen from a larger needle inner diameter of 12# as Fig. 5(a-e) shown, which was because the strength of the electric field would decreased with increasing the inner diameter of the needle, leading to the weaken of stretching force of jet by electrostatic field under the same spinning conditions, resulted in the increase of fiber diameter and the emergence of flat fiber.

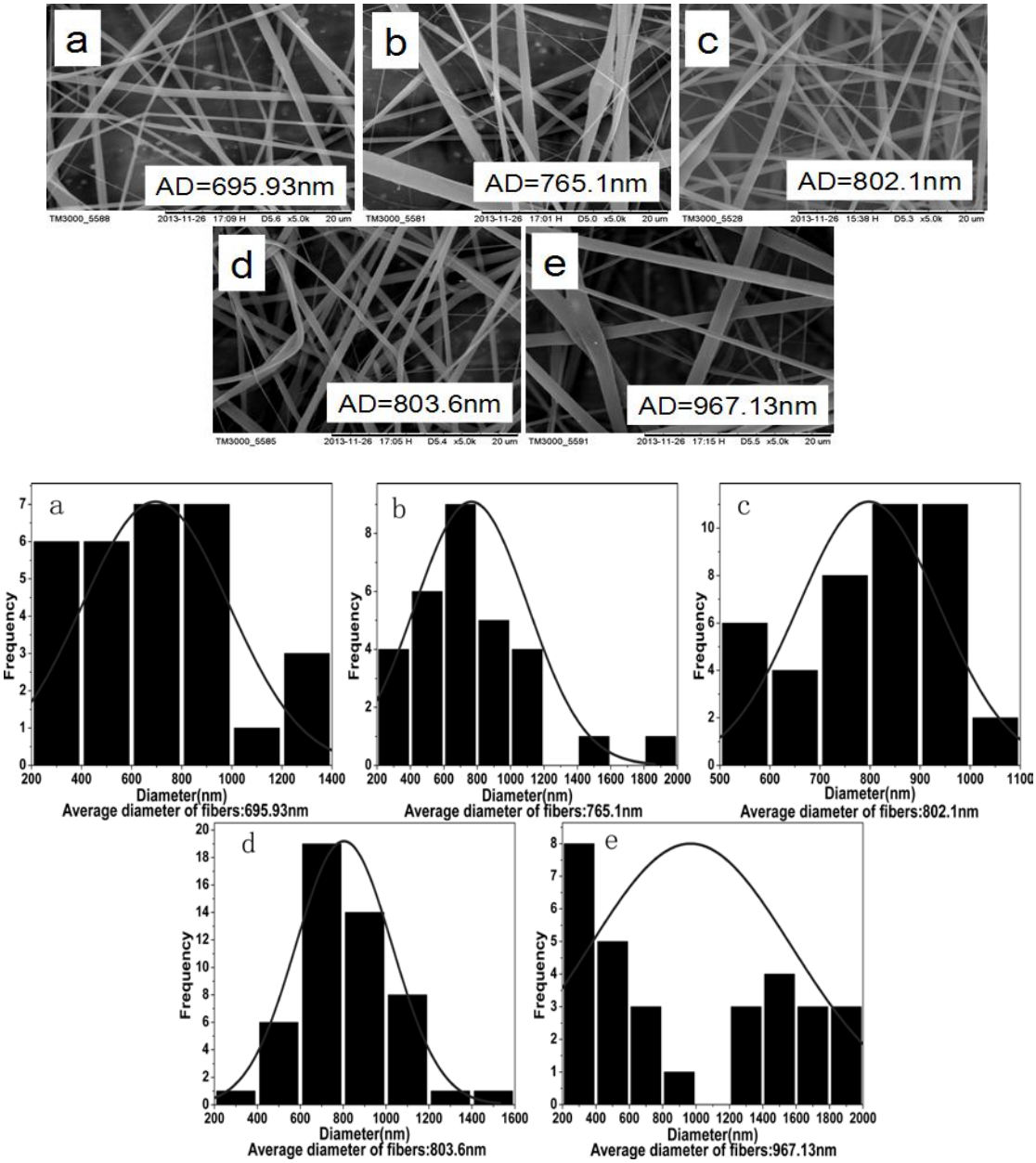

Fig. 5. SEM images and diameter distribution of KGM-g-St/BA fibers at various needle inner diameter (a) 6# , (b) 7#, (c) 8#, (d) 9#, (e) 12# ; 15 kV, 1 mL/h , 15 cm, 35 ºC.

3.2.5 Influence of the environment temperature on morphology of nanofibers

Fig. 6 showed the morphology and diameter distribution of KGM-g-St/BA fibers under different ambient temperature. It could be seen that with increasing the temperature in the range of 20 ºC to 30 ºC, the average fiber diameters decreased from 415.3 nm to 312.17 nm and the range of diameter distribution decreased from 200-900 nm to 200-700 nm, attributed to the faster evaporation of the solvent at increased temperature. The average fiber diameters increased from 312.17 nm to 676.43 nm and the range of diameter distribution increased from 200-1200 nm to 200-1800 nm with increasing the temperature ranging from 30 ºC to 50 ºC. This was probably due to that solvent trifluoroacetic acid was a kind of volatile matter, which accelerated the evaporation of solvent inside the syringe with an increase in temperature, resulting in an increase in the concentration of the solution and viscosity. We could see from the process of experiment that the solvent in the syringe would be quickly evaporated at the temperature of 50 ºC and the diameter distribution was broaden, therefore, the optimum temperature of KGM-g-St/BA electrospun fibers using trifluoroacetic acid as a solvent was 20-30 ºC.

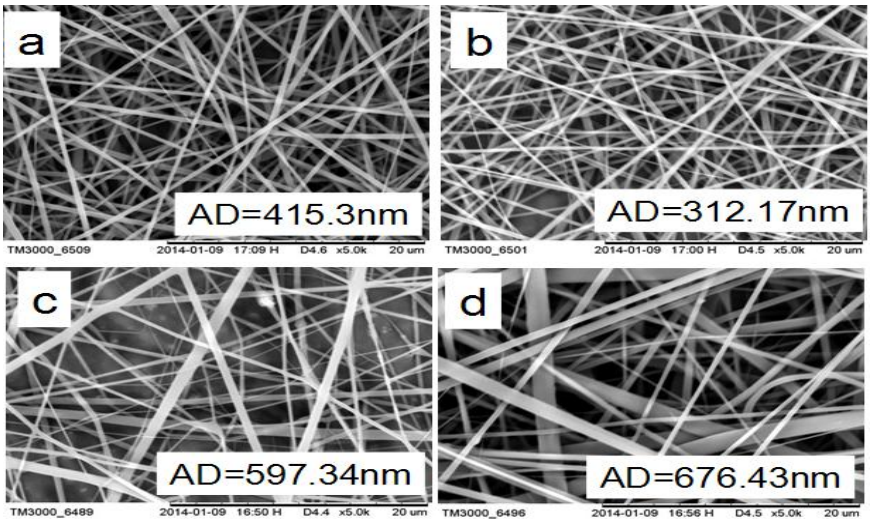

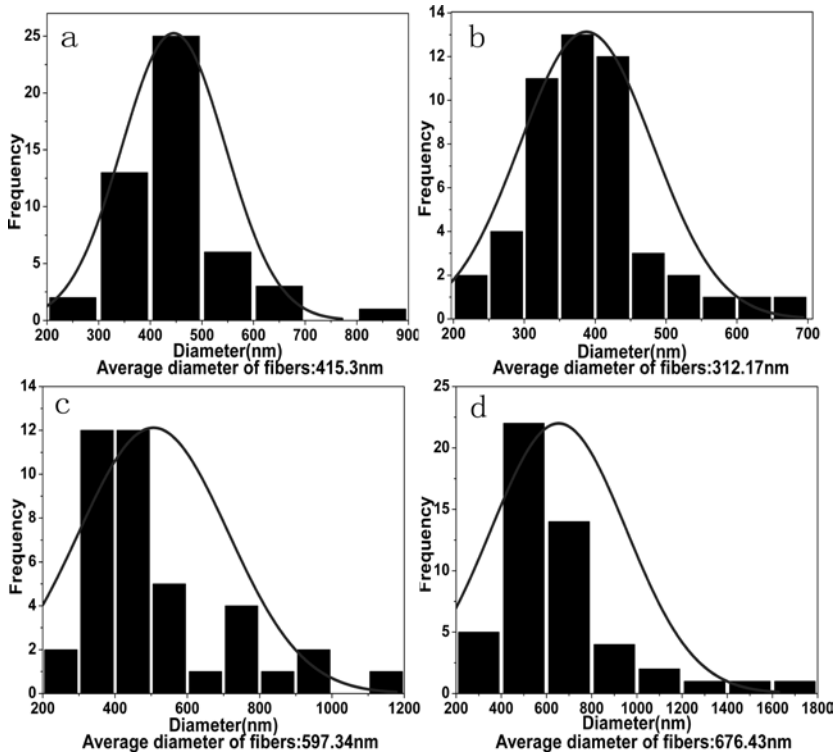

Fig. 6. SEM images and diameter distribution of KGM-g-St/BA fibers at various temperature (a) 20 ºC, (b) 30 ºC, (c) 40 ºC, (d) 50 ºC; 15 kV, 1 mL/h, 15 cm, 8#.

3.3 The core/shell structure of PCL/KGM-g-St/BA fibers

Fig. 7(a-b) showed the cross-sectional images of the core/shell PCL/KGM-g-St/BA single and multiple fibers, which displayed the presence of PCL polymer in the core section. And the core-shell structure of the fibers could be clearly seen by the section structure images. PCL in the core was very soft and not easy to break, and KGM-g-St/BA in the shell had a small tensile fracture strain, presented brittle fracture, which resulted in a complete fracture or only a shell fracture of the fiber when applying different levels of tensile force after put the fiber film into the liquid nitrogen.

Fig. 7(c-d) showed the TEM images of a bundle and a single of PCL/KGM-g-St/BA fibers, the core/shell structure could be clearly seen. The interface between KGM-g-St/Ba (shell) and PCL (core) was clear since the differences in structure and contrast between them. From the spinning process, it could be known that KGM-g-St/BA was the shell and PCL was the core. The SEM and TEM images (Fig. 7) confirmed that core/shell fibers of PCL/KGM-g-St/BA were successfully acquired by coaxial electrospinning.

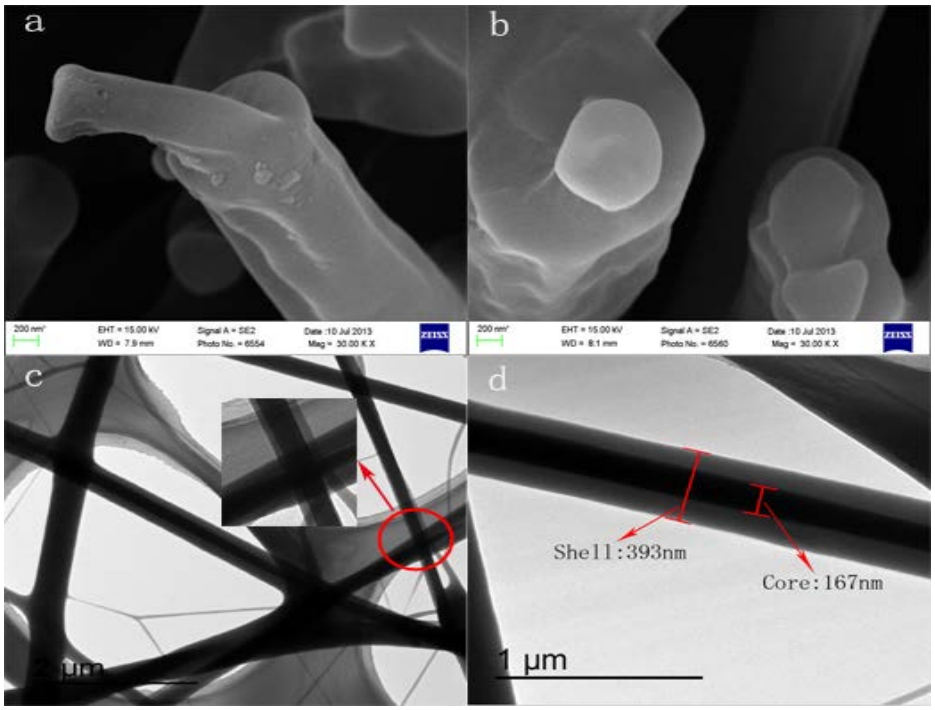

Fig. 7. (a-b) The SEM images of fracture surface of KGM-g-St/BA (shell)-PCL (core), (c) the TEM image of a bundle of KGM-g-St/BA (shell)-PCL(core) fibers and (d) the TEM image of a single of KGM-g-St/BA (shell)-PCL(core) fibers.

3.4 Hydrophobic performance analysis of KGM-St/BA and core/shell PCL/KGM-g-St/BA fiber films

Fig. 8(a-b) showed the SEM images and water-contact angle (WCA) measurements of KGM and KGM-g-St/BA disks. The WCA value of KGM disk, was 59.0 degrees (Fig. 8a), indicated that KGM was a kind of hydrophilic material, while a WCA value of KGM-g-St/BA disk increased to 92.04 degrees (Fig. 8b), revealed that the hydrophobic property of KGM was improved after grafting styrene and butyl acrylate. The WCA value of electrospun KGM-g-St/BA fiber film was 131.2 degrees (Fig. 8c), which contributed to the electrospun fibers with micro/nano multistage structure having a great surface roughness, leading to more air existing between fiber film and liquid. The coaxial electrospun core-shell fiber film showed a WCA value of 134.6 degrees (Fig. 8d), implied that it had a good hydrophobic surface characteristic, which was due to hydrophobic characteristic of both the KGM-g-St/BA and PCL.

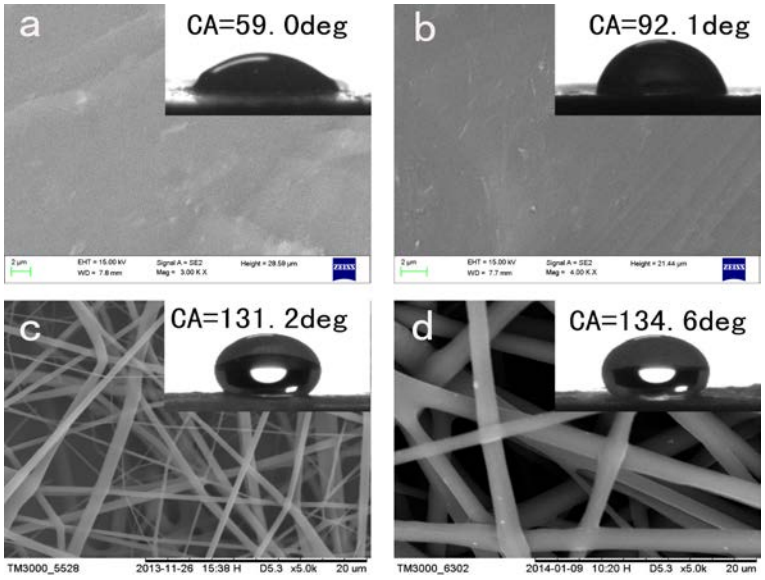

Fig. 8. SEM and contact angle of (a) KGM disk; (b) KGM-g-St/BA disk (c) KGM-g-St/BA cast film; (d) KGM-g-St/BA electrospun fiber film; (e) KGM-g-St/BA-PCL electrospun fiber film.

4 Conclusions

The spinnability of KGM was successfully improved through the synthesized KGM-g-St/BA copolymer via free-radical polymerization. Fibers of KGM-g-St/BA were obtained by electrospinning technique and core-shell PCL/KGM-g-St/BA fibers were obtained by coaxial electrospinning using KGM-g-St/BA as the shell and PCL as the core. The average diameter (AD) of fibers increased with the increasing of flow rate, needle tip to collector distance, the needle inner diameter and environment temperature ranged from 30 ºC to 50 ºC, however, the AD of fibers decreased with the increasing of applied voltage and environment temperature ranged from 20 ºC to 30 ºC. The hydrophobic property of KGM (59.0°) had dramatically increased via grafting modification. KGM-g-St/BA graft copolymer fiber film and core-shell fiber film have a good hydrophobic property with the contact angles of 131.2° and 134.6°, which could have a potential application in the field of hydrophobic materials. This research provided a new thought and method for the electrospinning preparation of composite fiber film of KGM-g-St/BA copolymer and PCL compound fiber film.

Acknowledgments

The authors thank the financial support from the Fruit Transformation Cultivation Project of Sichuan Province Education Department of China (No. 12zz005). We acknowledge the technology support of Engineering Research Center of Biomass Materials, Ministry of Education.

References

[1] Agarwala S, Greinera A, Wendorff J H. Functional materials by electrospinning of polymers, Prog. Polym. Sci. 38 (2013) 963-991.
[2] Geng X Y, Kwon O H, Jang J H. Electrospinning of chitosan dissolved in concentrated acetic acid solution, Biomaterials 26 (2005) 5427-5432.
[3] Song T, Zhang Y Z, Zhou T J, et al. Encapsulation of self-assembled FePt magnetic nanoparticles in PCL nanofibers by coaxial electrospinning, Chem. Phys. Lett. 415 (2005) 317-322.
[4] Qin X H, Wang S Y. Filtration properties of electrospinning nanofibers, J. Appl. Polym. Sci. 102 (2006) 1285-1920.
[5] Siró I, Plackett D. Microfibrillated cellulose and new nanocomposite materials: a review, Cellulose. 17 (2010) 459-494.
[6] Zahedi P, Rezaeian I, Ranaei-Siadat S O, et al. A review on wound dressings with an emphasis on electrospun nanofibrous polymeric bandages, Polym. Advan. Technol. 21 (2010) 77.
[7] Srinivasan G, The University of Akron 1994; Akron: 1–121.
[8] Yarin A L. Coaxial electrospinning and emulsion electrospinning of core–shell fibers, Polym. Advan.Technol. 22 (2011) 310-317.
[9] Forward K M, Flores A, Rutledge G C. Production of core/shell fibers by electrospinning from a free surface, Chem. Eng. Sci. 104 (2013) 250-259.
[10] Sun B, Duan B, Yuan X Y. Preparation of core/shell PVA/PLA ultrafine fibers by coaxial electrospinning, J. Appl. Polym. Sci. 102 (2006) 39-45.
[11] Zhang X, Thavasi V, Mhaisalkar S G, et al. Novel hollow mesoporous 1D TiO2 nanofibers as photovoltaic and photocatalytic materials, Nanoscale. 4 (2012) 1707-1716.
[12] Zhang X, Aravindan V, Kumar P S, et al. Synthesis of TiO 2 hollow nanofibers by co-axial electrospinning and its superior lithium storage capability in full-cell assembly with olivine phosphate, Nanoscale. 5 (2013) 5973-5980.
[13] Greiner A, Wendorff J H. Electrospinning: a fascinating method for the preparation of ultrathin fibers, Angew. Chem. Int. Ed. 46 (2007) 5670-5703.
[14] Lu J, Wang X D, Xiao C B. Preparation and characterization of konjac glucomannan/poly (diallydimethylammonium chloride) antibacterial blend films, Carbohyd. Polym. 73 (2008) 427-437.
[15] Xiong Z D, Zhou W Q, Sun L J, et al. Konjac glucomannan microspheres for low-cost desalting of protein solution, Carbohyd. Polym. 111 (2014) 56-62.
[16] Chen L G, Liu Z L, Zhuo R X. Synthesis and properties of degradable hydrogels of konjac glucomannan grafted acrylic acid for colon-specific drug delivery, Polymer 46 (2005) 6274-6281.
[17] Li J, Ye T, Wu X F, et al. Preparation and characterization of heterogeneous deacetylated konjac glucomannan, Food Hydrocolloid. 40 (2014) 9-15.
[18] Cheng L H, Abd Karim A, Norziah M H, et al. Modification of the microstructural and physical properties of konjac glucomannan-based films by alkali and sodium carboxymethylcellulose, Food Res. Int. 35 (2002) 829-836.
[19] Kobayashi S, Tsujihata S, Hibi N, et al. Preparation and rheological characterization of carboxymethyl konjac glucomannan, Food Hydrocolloid, 16 (2002) 289-294.
[20] Zhang Y Q, Xie B J, Gan X. Advance in the applications of konjac glucomannan and its derivatives, Carbohyd. Polym. 60 (2005) 27-31.
[21] Tatirat O, Charoenrein S, Kerr W L, Physicochemical properties of extrusion-modified konjac glucomannan, Carbohyd. Polym. 87 (2012) 1545-1551.
[22] Nie H, Shen X, Zhou Z, et al. Electrospinning and characterization of konjac glucomannan/chitosan nanofibrous scaffolds favoring the growth of bone mesenchymal stem cells, Carbohyd. Polym. 85 (2011) 681-686.
[23] Xu C G, Luo X G, Lin X Y, et al. Preparation and characterization of polylactide/thermoplastic konjac glucomannan blends, Polymer 50 (2009) 3698-3705.
[24] Gao S J, Zhang L N. Molecular weight effects on properties of polyurethane/nitrokonjac glucomannan semiinterpenetrating polymer networks, Macromolecules 34 (2001) 2202-2207.
[25] Luo X G, He P, Lin X Y. The mechanism of sodium promoting the gelation of konjac glucomannan (KGM), Food Hydrocolloid. 30 (2013) 92-99.
[26] Wang X, Guang S Y, Yan R W, et al. Controllable preparation and optical limiting properties of CdS

nanocomposites in KGM-AA soft template, Mater. Res. Bull. 48 (2013) 2469-2475.
[27] Kaur S, Ma Z, Gopal R, et al. Plasma-induced graft copolymerization of poly (methacrylic acid) on electrospun poly (vinylidene fluoride) nanofiber membrane, Langmuir. 23 (2007) 13085-13092.
[28] Chen H L, Huang J, Yu J H, et al. Electrospun chitosan-graft-poly (ε-caprolactone)/poly (ε-caprolactone) cationic nanofibrous mats as potential scaffolds for skin tissue engineering, Internat. J. boil. Macromol. 48 (2011) 13-19.
[29] Lin X Y, Li Y, Chen Z, et al. Synthesis, characterization and electrospinning of new thermoplastic carboxymethyl cellulose (TCMC), Chem. Eng. J. 215 (2013) 709-720.
[30] Wu K J, Wu C S, Chang J S. Biodegradability and mechanical properties of polycaprolactone composites encapsulating phosphate-solubilizing bacterium Bacillus sp. PG01, Process Biochem. 42 (2007) 669-675.
[31] Meng F B, Zheng L J, Wang Y H, et al. Preparation and properties of konjac glucomannan octenyl succinate modified by microwave method, Food Hydrocolloid. 38 (2014) 205-210.
[32] Wu C H, Peng S H, Wen C R, et al. Structural characterization and properties of konjac glucomannan/curdlan blend films, Carbohyd. Polym. 89 (2012) 497-503.
[33] Ferreira H P, Parra D F, Lugao A B. Radiation-induced grafting of styrene into poly(vinylidene fluoride) film by simultaneous method with two different solvents, Radiat. Phys. Chem. 81 (2012) 1341-1344.
[34] Zuber M, Shah S A A, Jamil T, et al. Performance behavior of biological macromolecules, Int. J. Biol. Macromol. 67 (2014) 254-259.
[35] Sill T J, von Recum H A. Electrospinning: applications in drug delivery and tissue engineering, Biomaterials 29 (2008) 1989-2006.
[36] Bhardwaj N, Kundu S C. Electrospinning: a fascinating fiber fabrication technique, Biotechnol. Adv. 28 (2010) 325-347.
[37] Ramakrishna S, Fujihara K, Teo W E, et al. An introduction to electrospinning and nanofibers, Singapore, 2005.